ABSENCE OF A METALLICITY EFFECT FOR ULTRA-SHORT-PERIOD PLANETS

Joshua N. Winn[1], Roberto Sanchis-Ojeda[2], Leslie Rogers[3], Erik A. Petigura[4], Andrew W. Howard[4], Howard Isaacson[2], Geoffrey W. Marcy[2], and Kevin Schlaufman[6]

[1]Department of Astrophysical Sciences, Princeton University, 4 Ivy Lane, Princeton, NJ 08544, USA

[2]Department of Astronomy, University of California, Berkeley, CA 94720

[3]Department of Astronomy & Astrophysics, University of Chicago, 5640 South Ellis Avenue, Chicago, IL 60637, USA

[4]Department of Astronomy, California Institute of Technology, Pasadena, CA 91125, USA

[6]Department of Physics and Astronomy, Johns Hopkins University, Baltimore, MD 21218, USA

ABSTRACT

Ultra-short-period (USP) planets are a newly recognized class of planets with periods shorter than one day, and radii smaller than about 2 $R_\oplus$. It has been proposed that USP planets are the solid cores of hot Jupiters that lost their gaseous envelopes due to photo-evaporation or Roche lobe overflow. We test this hypothesis by asking whether USP planets are associated with metal-rich stars, as has long been observed for hot Jupiters. In contrast, we find the metallicity distributions of USP and hot-Jupiter hosts to be significantly different ($p = 2 \times 10^{-4}$), based on Keck spectroscopy of *Kepler* stars. Evidently the sample of USP planets is not dominated by the evaporated cores of hot Jupiters. The metallicity distribution of USP hosts is indistinguishable from that of short-period planets with sizes between 2-4 $R_\oplus$. Thus it remains possible that the USP planets are the solid cores of formerly gaseous sub-Neptune planets.

Keywords: planetary systems—planets and satellites: detection, atmospheres

1. INTRODUCTION

The discovery of planets with orbital periods shorter than one day, and comparable in size to the Earth, has sparked discussion about their origin and evolution. The first well-documented planets in this category were CoRoT-7b (Léger et al. 2009), Kepler-10b (Batalha et al. 2011), 55 Cnc e (Dawson & Fabrycky 2010; Winn et al. 2011; Demory et al. 2011), and Kepler-78b (Sanchis-Ojeda et al. 2013). A sample of about 100 such planets was drawn together and analyzed by Sanchis-Ojeda et al. (2014). An independent *Kepler* survey was performed by (Jackson et al. 2013), and new examples have since been discovered by Becker et al. (2015), Adams et al. (2016), and Vanderburg et al. (2016).

Among the hypotheses for the origin of these "ultra-short-period" (USP) planets is that they are the exposed solid cores of hot Jupiters that formed through core accretion. As circumstantial evidence for a connection between USPs and hot Jupiters, Sanchis-Ojeda et al. (2014) and Steffen & Coughlin (2016) noted that these two categories of planets are both found around ≈0.5% of FGK stars. They also found that USP planets are almost always smaller than 2 $R_\oplus$, putting them in or near the size range for which planets are thought to have a mainly rocky composition (Weiss & Marcy 2014; Rogers 2015). They hypothesized that the most strongly irradiated hot Jupiters eventually lose their gaseous envelopes due to photo-evaporation, or Roche lobe overflow (Valsecchi et al. 2014). This would leave behind a nearly-naked core in

a close-in orbit. Proving this hypothesis to be correct would confirm the core-accretion theory, and enable direct measurements of the size and mass distribution of the rocky cores that nucleate the growth of giant planets.

However, there are other possibilities for the origin of the USP planets. They might represent the short-period extension of the distribution of close-in rocky planets which either formed by core accretion in their current orbits (Chiang & Laughlin 2013), or migrated inwards from more distant orbits (Ida & Lin 2004; Schlaufman et al. 2010; Terquem 2014). Another possibility is that the USP planets are the exposed remnants not of hot Jupiters, but of smaller gaseous planets with sizes between 2-4 $R_\oplus$ (Lundkvist et al. 2016; Lee & Chiang 2017).

Here we test for a connection between USPs and hot Jupiters based on the metallicities of the host stars. It has long been known that stars with close-in giant planets have systematically higher metallicities than randomly chosen stars in the solar neighborhood (Gonzalez 1997; Santos et al. 2004; Fischer & Valenti 2005). In contrast, the host stars of smaller planets show little if any association with high metallicity (Udry et al. 2006; Schlaufman & Laughlin 2011; Buchhave et al. 2012) [although we note that these studies focused on stars near solar metallicity, and that Zhu et al. (2016) have questioned some of the evidence]. If all USP planets are the cores of former hot Jupiters, we should observe similar metallicity distributions for USP and hot-Jupiter hosts. If in-
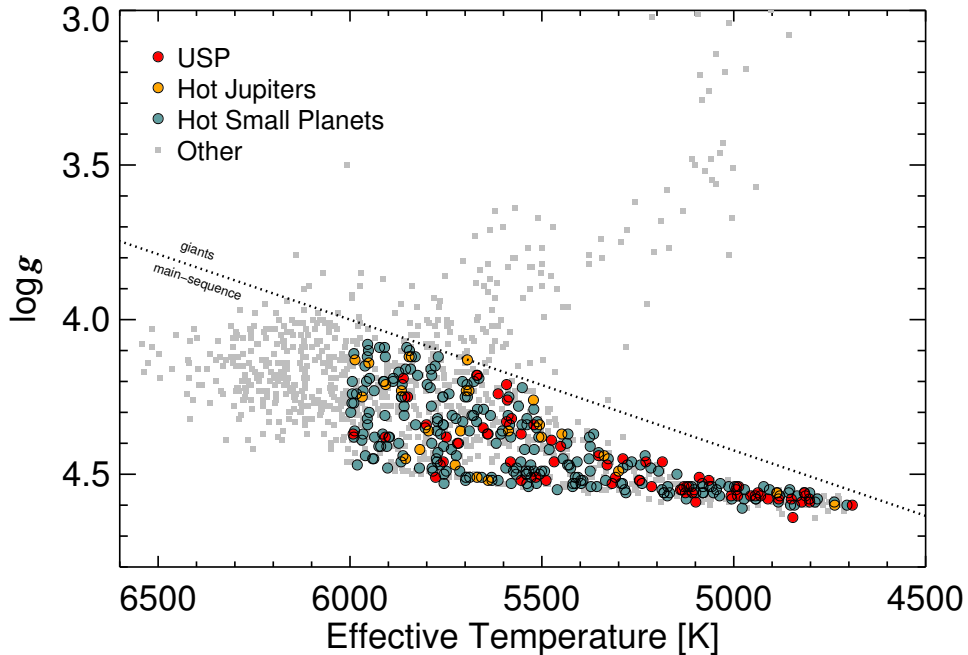
Figure 1. **Spectroscopic parameters of the stellar samples.** Stars below the dashed line were deemed main-sequence stars for the purpose of constructing our statistical samples, as described in §3. Colored circles show the parameters of the sample stars; the smaller squares are for the broader sample of stars in the California *Kepler* Survey (Petigura et al. 2017).

stead USPs arise from evaporation of smaller planets, or if they form in the same way as somewhat longer-period planets, then the USP host stars would have a metallicity distribution similar to that of short-period sub-Neptunes.

The metallicity distribution of *Kepler* planet hosts has been investigated previously by Buchhave et al. (2012); Mann et al. (2013); Buchhave et al. (2014); Dong et al. (2014); Schlaufman (2015); Buchhave & Latham (2015); Guo et al. (2016) and Mulders et al. (2016), but without special attention to USP hosts. This study focuses on USP planets, using the curated sample of Sanchis-Ojeda et al. (2014), and metallicities from new high-resolution spectroscopy by Petigura et al. (2017). Section 2 describes our observations and sample selection. Section 3 compares the metallicity distributions of the host stars of hot Jupiters, sub-Neptunes, and USP planets. Section 5 provides some concluding remarks.

2. OBSERVATIONS AND SAMPLE SELECTION

Sanchis-Ojeda et al. (2014; hereafter, SO+14) presented a catalog of USP planet candidates. We performed high-resolution optical spectroscopy of 71 of the stars in this sample with the Keck I telescope and HIRES (Vogt et al. 1994), as part of the larger California Kepler Survey (Petigura et al. 2017). All the stars brighter than $m_{Kep} = 15.3$ were observed. Some fainter stars were also observed, particularly those hosting the planets with the shortest orbital periods. The spectra were collected from 2013 June to 2014 September. We used the standard California Planet Search setup, but without the iodine cell, giving a typical spectral resolu-

tion of $R = 60,000$ over the wavelength range 0.36-0.80 μm. The exposure times were typically 10 minutes, with a maximum exposure time of 20 minutes. For stars brighter than $m_{Kep} = 14.3$, we achieved a signal-to-noise ratio (SNR) of 40 pixel^{-1} at 0.55 μm. For fainter stars, the SNR was between 20-40 pixel^{-1}.

The spectroscopic parameters of each star were determined with a combination of `SpecMatch`, a template-matching code, and a variant of SME, a spectral synthesis code. Details are provided by Petigura et al. (2017), who demonstrated a precision of 60 K in effective temperature, 0.07 dex in surface gravity, 0.04 dex in [Fe/H].

For our study we omitted stars with $T_{eff} < 4700$ K. There are severe discrepancies between the synthesized and observed spectra for such cool stars, due to the onset of molecular absorption that is poorly treated in the Coelho et al. (2005) models. We also removed KOI 2813 and KIC 5955905, for which the apparent transit signals have been shown to be caused by binary stars rather than transiting planets.[1]

The mass and radius of each star were determined by Johnson et al. (2017), by comparing the observed spectroscopic parameters with those calculated with the Dartmouth stellar-evolutionary models (Dotter et al. 2008), using the

---

[1] KOI 2813 was identified as a probable spectroscopic binary by Kolbl et al. (2015). KIC 5955905 is a probable background binary, based on observations of large chromatic variations in the apparent transit depth (E. Palle, private communication).
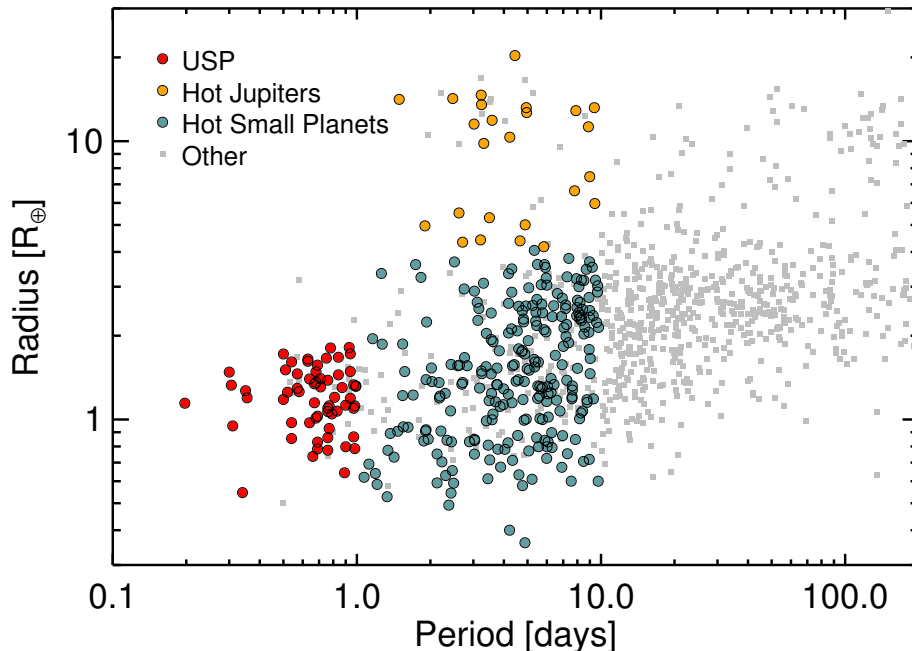
Figure 2. **Orbital period and planetary radius.** The colored circles show our statistical samples; the smaller squares are for the broader sample of stars in the California *Kepler* Survey (Petigura et al. 2017).

`isochrones` code (Morton et al. 2016)[2]. The inputs were $T_{\rm eff}$, $\log g$, and [Fe/H], along with their associated uncertainties. The code produces *a posteriori* distributions for the stellar mass, radius, and age, by interpolating between the available Dartmouth models. The radii of the transiting planets were then calculated from the stellar radii and the measured transit depths.

3. METALLICITY DISTRIBUTIONS

We wanted to compare the metallicity distribution of the USP host stars to that of hot Jupiters, and of smaller planets. To construct the appropriate samples we drew on the preceding results for the USP host stars, as well as the rest of the stars in the California *Kepler* Survey (Petigura et al. 2017). The larger sample includes about 1000 stars selected from the list of *Kepler* Objects of Interest (KOI), spanning a wide range of stellar types, planet sizes, and orbital periods. The stars were selected for spectroscopy independently of metallicity. Indeed, little information was available about the metallicities prior to the observations.

We restricted our attention to main-sequence stars in the temperature range 4700-6000 K, in which almost all of the USP planet hosts reside. We constructed three samples:

1. *USPs*: Stars having a planet with orbital period shorter than 1 day, selected from SO14 as described above. This sample has 62 stars.

2. *Hot Jupiters*: Stars from the sample of Petigura et al. (2017) with a planet larger than 4 $R_\oplus$ and an orbital period shorter than 10 days. We omitted objects designated as "False Positive" in the Q1-17 KOI list of Twicken et al. (2016), or in the spectroscopic follow-up program of Santerne et al. (2016). We also omitted objects with inferred sizes larger than 20 $R_\oplus$ because experience has shown that in these cases the transit-like signal arises from a binary star rather than a transiting planet. This sample has 25 stars.

3. *Hot Small Planets*: Stars with planets smaller than 4 $R_\oplus$ and orbital periods between 1-10 days, after omitting objects designated as "False Positives". There are 242 stars in this sample.

Tables 1 and 2 give the pertinent properties of the USP and hot Jupiter hosts. Figure 1 shows the spectroscopic parameters $T_{\rm eff}$ and $\log g$ for the stars in each sample. The dashed line is the boundary we used to identify main-sequence stars; our samples were restricted to stars below this line. Figure 2 shows the period-radius distribution of the planets hosted by the stars in each sample. In both figures, the small gray squares show the full sample of *Kepler* stars that were analyzed by Johnson et al. (2017).

Figure 3 focuses exclusively on the USP sample. Note in particular that all of the USP planets have sizes $\lesssim 2\,R_\oplus$, even though no selection was made based on planet size. Thus, we confirm the finding of SO+14 that USP planets are almost always smaller than 2 $R_\oplus$. We find no major differences be-

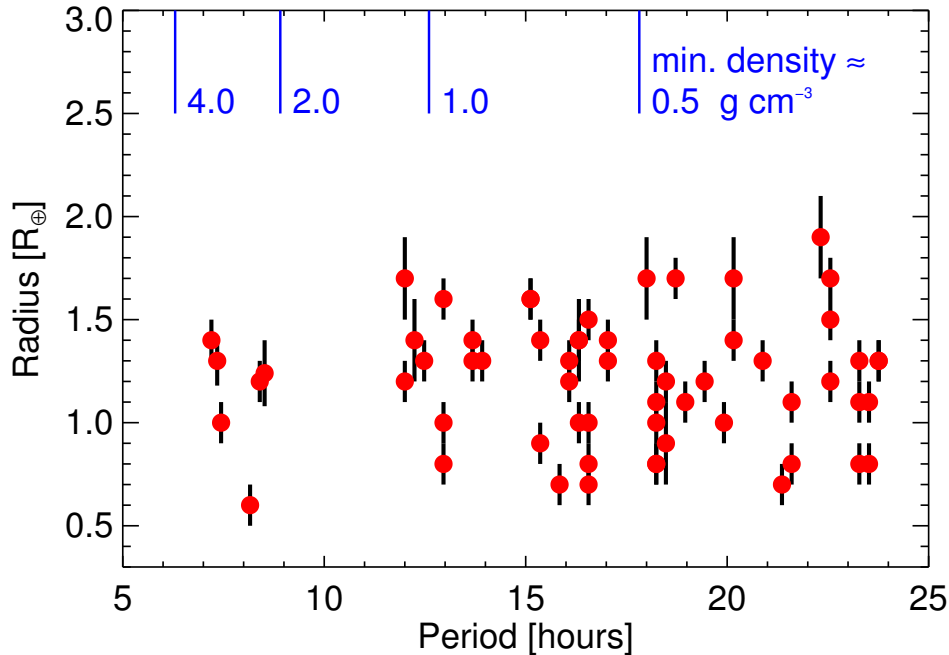[2] https://github.com/timothydmorton/isochrones (version 1.0)

Figure 3. **Orbital period and planetary radius for USPs.** A closer look at the radii and periods of the planets in the USP sample. Also marked are the Roche-limiting minimum periods for incompressible fluid bodies with mean densities of 0.5, 1.0, 2.0, and 4.0 g cm^{-3}, using Eqn. (2) of Rappaport et al. (2013). In reality, compression of the planetary interior may lower the minimum period by as much as $\approx 15\%$.

tween our newly-determined radius distribution for the USP planets, and the distribution presented by SO+14, except that the new estimates of planetary radii have smaller uncertainties, and two outliers with sizes $> 2.5\,R_\oplus$ do not appear in the new sample.

Figure 4 shows the distribution of [Fe/H] for the stars in each sample. Even at a glance, the Hot Jupiters are seen to be weighted toward higher [Fe/H] than both the USP and the Hot Small Planets. The distributions for the USP and Hot Small Planets appear similar to one another. To quantify these impressions we performed two-sample Kolmogorov-Smirnov tests, which estimate the probability p that two samples are drawn from the same distribution. The results, given in Table 3, indicate that the USP and Hot Jupiters are very unlikely to be drawn from the same sample, while the USPs and the Hot Smaller Planets have distributions that are indistinguishable with the present data.

4. UPPER BOUND ON HOT-JUPITER FRACTION

Evidently the USP host stars have a different metallicity distribution than the hot Jupiter hosts. We placed an upper bound on the fraction f of members in the USP sample that could have been drawn from the same distribution as the Hot Jupiter sample, using a Monte Carlo technique. We consider the range of f from zero to unity. For each choice of f, we construct a sample of 62 metallicities (matching the actual USP sample size), by randomly drawing $[62f]$ values from the USP sample, and $62 - [62f]$ values from the hot Jupiter sample, where $[x]$ indicates rounding to the nearest integer.

We add Gaussian errors to each metallicity with a standard deviation of 0.04. We then compute the probability p that the simulated sample is drawn from the same underlying distribution as the Hot Jupiters, using a two-sided Kolmogorov-Smirnov test. We repeat this procedure 10^3 times and record the mean p value.

For low values of f, the simulated sample is drawn entirely from the USPs and the p-values are $\sim 10^{-4}$ as described in the previous section. For values of f approaching unity, the p-values are ~ 1 because the Hot Jupiter sample is being compared with itself. To determine an upper bound on f, we sought the value for which $p = 0.0455$, corresponding to a traditional 2σ level of confidence. The result is $f < 0.46$, implying that no more than about half of the metallicities of the USP host stars could have been drawn from the same metallicity distribution as the hot-Jupiter hosts.

5. CONCLUSIONS

The metallicity distribution of the USP host stars does not resemble the metallicity distribution of hot-Jupiter host stars. In particular, the USP host stars show no evidence for an association with high metallicity, in contrast with the hot Jupiters. The USP hosts have a mean metallicity near the Sun's value, and similar to that of the general planet-hosting population of *Kepler* stars.

We interpret this result as an argument against any theory in which most of the USPs are descended from hot Jupiters. In such a theory, the stars that are currently observed to have USPs were once hosts to hot Jupiters, and their metallicity
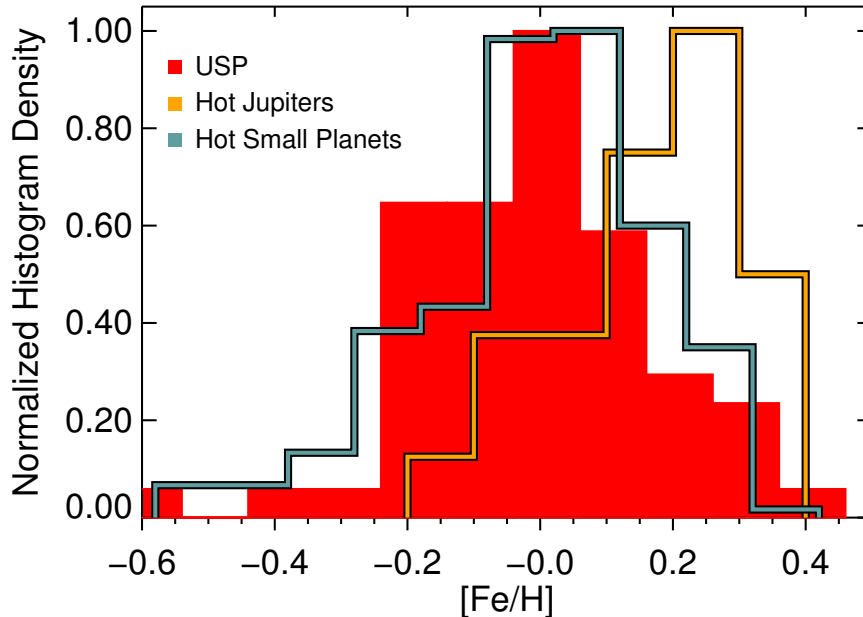
Figure 4. **Metallicity distributions** of the three statistical samples. The hot-Jupiter hosts have a different metallicity distribution (more weighted toward high metallicity) from the USP hosts, and from the hosts of close-in planets smaller than Neptune.

distribution should be the same as those stars currently observed to have hot Jupiters. The only way we see to escape this conclusion—which seems very unlikely—is to hypothesize that the process that converts hot Jupiters into USPs also systematically lowers the metallicity of the host star by $\Delta[Fe/H] \sim -0.1$, so as to match the metallicity distribution of the hosts of smaller *Kepler* planets.

The possibility that USPs represent the solid cores of erstwhile hot Jupiters had already been deemed unlikely on theoretical grounds, because of the difficulty of removing such a massive gaseous atmosphere. Murray-Clay et al. (2009) modeled the wind launched from a gaseous planet by a star's high-energy radiation, and found it difficult to erode the entire atmosphere of a hot Jupiter. Our work has provided empirical support for this conclusion.

It remains plausible that USPs are the solid cores of what were once Neptune-sized or smaller planets. This is also compatible with the tendency of USPs to have sub-Neptune companion in somewhat wider orbits (Sanchis-Ojeda et al. 2014; Adams et al. 2016). Multiple theoretical studies have shown that it is possible to lose most of the gas from a low-density planet smaller than Neptune(Howe & Burrows 2015; Lopez 2016; Jackson et al. 2017; Ginzburg & Sari 2016). Also consistent with this picture is the recent discovery by Fulton et al. (2017) that relatively few *Kepler* planets have sizes between 1.5-2 $R_\oplus$. The missing planets in this size range might have been gaseous sub-Neptunes whose atmospheres were stripped.

The USPs remain an attractive subject for future work to understand their origin, occurrence rate, radius distribution, and the dependence of all these quantities on the properties of the host star. The current sample of ~ 100 have apparent magnitudes that are generally too faint for precise Doppler monitoring, observations of the Rossiter-McLaughlin effect, and detections of occultations or transmission effects. The *TESS* mission (Ricker et al. 2015) will help to remedy this problem by searching a similar number of stars as the *Kepler* mission, but brighter by several magnitudes.

REFERENCES

Adams, E. R., Jackson, B., & Endl, M. 2016, AJ, 152, 47

Batalha, N. M., Borucki, W. J., Bryson, S. T., et al. 2011, ApJ, 729, 27

Becker, J. C., Vanderburg, A., Adams, F. C., Rappaport, S. A., & Schwengeler, H. M. 2015, ApJL, 812, L18

Buchhave, L. A., & Latham, D. W. 2015, ApJ, 808, 187

Buchhave, L. A., Latham, D. W., Johansen, A., et al. 2012, Nature, 486, 375

Buchhave, L. A., Bizzarro, M., Latham, D. W., et al. 2014, Nature, 509, 593

Chiang, E., & Laughlin, G. 2013, MNRAS, 431, 3444

Coelho, P., Barbuy, B., Meléndez, J., Schiavon, R. P., & Castilho, B. V. 2005, A&A, 443, 735

Dawson, R. I., & Fabrycky, D. C. 2010, ApJ, 722, 937

Demory, B.-O., Gillon, M., Deming, D., et al. 2011, A&A, 533, A114

Dong, S., Zheng, Z., Zhu, Z., et al. 2014, ApJL, 789, L3

Dotter, A., Chaboyer, B., Jevremović, D., et al. 2008, ApJS, 178, 89

Fischer, D. A., & Valenti, J. 2005, ApJ, 622, 1102

Fulton, B. J., Petigura, E. A., Howard, A. W., et al. 2017, ArXiv e-prints, arXiv:1703.10375 [astro-ph.EP]

Ginzburg, S., & Sari, R. 2016, ArXiv e-prints, arXiv:1611.09373 [astro-ph.EP]

Gonzalez, G. 1997, MNRAS, 285, 403

Guo, X., Johnson, J. A., Mann, A. W., et al. 2016, ArXiv e-prints, arXiv:1612.01616 [astro-ph.SR]

Howe, A. R., & Burrows, A. 2015, ApJ, 808, 150

Ida, S., & Lin, D. N. C. 2004, ApJ, 616, 567

Jackson, B., Arras, P., Penev, K., Peacock, S., & Marchant, P. 2017, ApJ, 835, 145

Jackson, B., Stark, C. C., Adams, E. R., Chambers, J., & Deming, D. 2013, ApJ, 779, 165

Johnson, J. A., Petigura, E. A., Fulton, B. J., et al. 2017, ArXiv e-prints, arXiv:1703.10402 [astro-ph.EP]

Kolbl, R., Marcy, G. W., Isaacson, H., & Howard, A. W. 2015, AJ, 149, 18

Lee, E. J., & Chiang, E. 2017, ArXiv e-prints, arXiv:1702.08461 [astro-ph.EP]

Léger, A., Rouan, D., Schneider, J., et al. 2009, A&A, 506, 287

Lopez, E. D. 2016, ArXiv e-prints, arXiv:1610.01170 [astro-ph.EP]

Lundkvist, M. S., Kjeldsen, H., Albrecht, S., et al. 2016, Nature Communications, 7, 11201

Mann, A. W., Gaidos, E., Kraus, A., & Hilton, E. J. 2013, ApJ, 770, 43

Morton, T. D., Bryson, S. T., Coughlin, J. L., et al. 2016, ApJ, 822, 86

Mulders, G. D., Pascucci, I., Apai, D., Frasca, A., & Molenda-Żakowicz, J. 2016, AJ, 152, 187

Murray-Clay, R. A., Chiang, E. I., & Murray, N. 2009, ApJ, 693, 23

Petigura, E. A., Howard, A. W., Marcy, G. W., et al. 2017, ArXiv e-prints, arXiv:1703.10400 [astro-ph.EP]

Rappaport, S., Sanchis-Ojeda, R., Rogers, L. A., Levine, A., & Winn, J. N. 2013, ApJL, 773, L15

Ricker, G. R., Winn, J. N., Vanderspek, R., et al. 2015, Journal of Astronomical Telescopes, Instruments, and Systems, 1, 014003

Rogers, L. A. 2015, ApJ, 801, 41

Sanchis-Ojeda, R., Rappaport, S., Winn, J. N., et al. 2014, ApJ, 787, 47

—. 2013, ApJ, 774, 54

Santerne, A., Moutou, C., Tsantaki, M., et al. 2016, A&A, 587, A64

Santos, N. C., Israelian, G., & Mayor, M. 2004, A&A, 415, 1153

Schlaufman, K. C. 2015, ApJL, 799, L26

Schlaufman, K. C., & Laughlin, G. 2011, ApJ, 738, 177

Schlaufman, K. C., Lin, D. N. C., & Ida, S. 2010, ApJL, 724, L53

Steffen, J. H., & Coughlin, J. L. 2016, Proceedings of the National Academy of Science, 113, 12023

Terquem, C. 2014, MNRAS, 444, 1738

Twicken, J. D., Jenkins, J. M., Seader, S. E., et al. 2016, AJ, 152, 158

Udry, S., Mayor, M., Benz, W., et al. 2006, A&A, 447, 361

Valsecchi, F., Rasio, F. A., & Steffen, J. H. 2014, ApJL, 793, L3

Vanderburg, A., Bieryla, A., Duev, D. A., et al. 2016, ApJL, 829, L9

Vogt, S. S., Allen, S. L., Bigelow, B. C., et al. 1994, in Proc. SPIE, Vol. 2198, Instrumentation in Astronomy VIII, ed. D. L. Crawford & E. R. Craine, 362

Weiss, L. M., & Marcy, G. W. 2014, ApJL, 783, L6

Winn, J. N., Matthews, J. M., Dawson, R. I., et al. 2011, ApJL, 737, L18

Zhu, W., Wang, J., & Huang, C. 2016, ApJ, 832, 196

Table 1. Characteristics of "USP" sample

ID	$T_{\rm eff}$ [K][a]	$\log g$[a]	[Fe/H][a]	$R_\star$ [$R_\odot$]	$M_\star$ [$M_\odot$]	R_p [$R_\oplus$]	$P_{\rm orb}$ [hr]
K00072	5614^{+63}_{-65}	$4.240^{+0.080}_{-0.130}$	$-0.150^{+0.040}_{-0.040}$	$1.210^{+0.140}_{-0.040}$	$0.920^{+0.050}_{-0.040}$	$1.70^{+0.20}_{-0.20}$	20.2
K00191	5451^{+63}_{-61}	$4.410^{+0.070}_{-0.070}$	$0.040^{+0.040}_{-0.070}$	$0.970^{+0.080}_{-0.040}$	$0.890^{+0.040}_{-0.040}$	$1.40^{+0.10}_{-0.10}$	17.0
K00500	4691^{+66}_{-64}	$4.600^{+0.030}_{-0.030}$	$0.030^{+0.040}_{-0.030}$	$0.720^{+0.060}_{-0.050}$	$0.750^{+0.040}_{-0.040}$	$1.30^{+0.10}_{-0.10}$	23.8
K00577	5090^{+65}_{-66}	$4.510^{+0.030}_{-0.040}$	$0.050^{+0.040}_{-0.040}$	$0.830^{+0.070}_{-0.060}$	$0.820^{+0.040}_{-0.040}$	$0.90^{+0.10}_{-0.10}$	15.4
K00717	5592^{+67}_{-68}	$4.210^{+0.080}_{-0.080}$	$0.270^{+0.040}_{-0.040}$	$1.310^{+0.140}_{-0.130}$	$1.020^{+0.050}_{-0.050}$	$0.80^{+0.10}_{-0.10}$	21.6
K01128	5352^{+58}_{-61}	$4.440^{+0.070}_{-0.070}$	$-0.090^{+0.040}_{-0.040}$	$0.910^{+0.080}_{-0.070}$	$0.840^{+0.040}_{-0.040}$	$1.30^{+0.10}_{-0.10}$	23.3
K01150	5801^{+65}_{-66}	$4.340^{+0.080}_{-0.070}$	$0.070^{+0.040}_{-0.040}$	$1.120^{+0.110}_{-0.100}$	$1.020^{+0.050}_{-0.050}$	$1.00^{+0.10}_{-0.10}$	16.3
K01169	5653^{+67}_{-66}	$4.350^{+0.080}_{-0.080}$	$0.080^{+0.040}_{-0.040}$	$1.090^{+0.100}_{-0.090}$	$0.970^{+0.050}_{-0.050}$	$1.50^{+0.10}_{-0.10}$	16.6
K01239	5749^{+65}_{-65}	$4.380^{+0.070}_{-0.070}$	$-0.110^{+0.040}_{-0.040}$	$1.040^{+0.080}_{-0.080}$	$0.940^{+0.040}_{-0.040}$	$1.70^{+0.10}_{-0.10}$	18.7
K01300	4813^{+65}_{-65}	$4.570^{+0.030}_{-0.030}$	$-0.000^{+0.040}_{-0.040}$	$0.740^{+0.060}_{-0.060}$	$0.760^{+0.040}_{-0.040}$	$1.60^{+0.10}_{-0.10}$	15.1
K01360	4911^{+67}_{-66}	$4.580^{+0.020}_{-0.030}$	$-0.250^{+0.040}_{-0.040}$	$0.710^{+0.060}_{-0.050}$	$0.710^{+0.040}_{-0.040}$	$0.80^{+0.10}_{-0.10}$	18.2
K01367	4956^{+65}_{-65}	$4.570^{+0.030}_{-0.040}$	$-0.160^{+0.040}_{-0.040}$	$0.740^{+0.060}_{-0.050}$	$0.750^{+0.040}_{-0.040}$	$1.40^{+0.10}_{-0.10}$	13.7
K01428	4823^{+64}_{-65}	$4.590^{+0.030}_{-0.040}$	$-0.180^{+0.040}_{-0.040}$	$0.710^{+0.060}_{-0.050}$	$0.720^{+0.040}_{-0.040}$	$1.90^{+0.20}_{-0.20}$	22.3
K01442	5592^{+62}_{-56}	$4.330^{+0.070}_{-0.090}$	$0.380^{+0.040}_{-0.040}$	$1.150^{+0.120}_{-0.110}$	$1.050^{+0.050}_{-0.050}$	$1.30^{+0.10}_{-0.10}$	16.1
K01655	5521^{+66}_{-65}	$4.340^{+0.080}_{-0.070}$	$-0.140^{+0.040}_{-0.040}$	$1.040^{+0.110}_{-0.100}$	$0.870^{+0.040}_{-0.040}$	$1.50^{+0.10}_{-0.10}$	22.6
K01875	5590^{+64}_{-63}	$4.260^{+0.080}_{-0.070}$	$-0.190^{+0.040}_{-0.040}$	$1.150^{+0.130}_{-0.120}$	$0.890^{+0.040}_{-0.040}$	$1.60^{+0.10}_{-0.10}$	13.0
K02039	5554^{+64}_{-64}	$4.520^{+0.040}_{-0.020}$	$0.190^{+0.040}_{-0.040}$	$0.910^{+0.070}_{-0.070}$	$0.990^{+0.050}_{-0.050}$	$0.80^{+0.10}_{-0.10}$	18.2
K02079	5475^{+66}_{-67}	$4.390^{+0.080}_{-0.080}$	$0.360^{+0.040}_{-0.040}$	$1.050^{+0.100}_{-0.090}$	$0.990^{+0.050}_{-0.050}$	$0.70^{+0.10}_{-0.10}$	16.6
K02093	5992^{+65}_{-64}	$4.370^{+0.070}_{-0.070}$	$-0.040^{+0.040}_{-0.040}$	$1.110^{+0.090}_{-0.090}$	$1.060^{+0.050}_{-0.050}$	$1.30^{+0.10}_{-0.10}$	23.8

Table 1 *(continued)*

ID	$T_{\rm eff}$ [K][a]	$\log g$[a]	[Fe/H][a]	$R_\star$ [$R_\odot$]	$M_\star$ [$M_\odot$]	R_p [$R_\oplus$]	$P_{\rm orb}$ [hr]
K02119	5139^{+66}_{-67}	$4.550^{+0.050}_{-0.030}$	$0.140^{+0.040}_{-0.040}$	$0.820^{+0.070}_{-0.060}$	$0.860^{+0.040}_{-0.040}$	$1.30^{+0.10}_{-0.10}$	13.7
K02202	5308^{+66}_{-65}	$4.510^{+0.060}_{-0.040}$	$0.290^{+0.040}_{-0.040}$	$0.890^{+0.070}_{-0.070}$	$0.940^{+0.050}_{-0.050}$	$1.20^{+0.10}_{-0.10}$	19.4
K02248	5130^{+64}_{-65}	$4.540^{+0.040}_{-0.040}$	$0.040^{+0.040}_{-0.040}$	$0.820^{+0.070}_{-0.060}$	$0.830^{+0.040}_{-0.040}$	$1.10^{+0.10}_{-0.10}$	18.2
K02250	4944^{+64}_{-68}	$4.570^{+0.040}_{-0.030}$	$0.040^{+0.040}_{-0.040}$	$0.770^{+0.060}_{-0.060}$	$0.800^{+0.040}_{-0.040}$	$1.60^{+0.10}_{-0.10}$	15.1
K02281	5065^{+65}_{-67}	$4.520^{+0.030}_{-0.050}$	$0.110^{+0.040}_{-0.040}$	$0.820^{+0.070}_{-0.060}$	$0.820^{+0.040}_{-0.040}$	$0.90^{+0.20}_{-0.20}$	18.5
K02393	4883^{+65}_{-66}	$4.580^{+0.030}_{-0.030}$	$-0.100^{+0.040}_{-0.040}$	$0.730^{+0.060}_{-0.050}$	$0.750^{+0.040}_{-0.040}$	$1.20^{+0.10}_{-0.10}$	18.5
K02396	5246^{+65}_{-66}	$4.520^{+0.050}_{-0.050}$	$0.060^{+0.040}_{-0.040}$	$0.850^{+0.070}_{-0.060}$	$0.860^{+0.040}_{-0.040}$	$1.70^{+0.20}_{-0.20}$	12.0
K02409	4846^{+65}_{-67}	$4.640^{+0.010}_{-0.010}$	$-0.640^{+0.040}_{-0.040}$	$0.630^{+0.050}_{-0.050}$	$0.620^{+0.040}_{-0.030}$	$1.30^{+0.10}_{-0.10}$	13.9
K02492	5668^{+58}_{-57}	$4.180^{+0.080}_{-0.100}$	$-0.370^{+0.040}_{-0.040}$	$1.230^{+0.150}_{-0.140}$	$0.830^{+0.040}_{-0.040}$	$1.10^{+0.10}_{-0.10}$	23.5
K02517	5582^{+64}_{-66}	$4.460^{+0.070}_{-0.070}$	$-0.160^{+0.040}_{-0.040}$	$0.920^{+0.070}_{-0.070}$	$0.880^{+0.040}_{-0.040}$	$1.10^{+0.10}_{-0.10}$	23.3
K02571	5317^{+64}_{-65}	$4.530^{+0.050}_{-0.030}$	$0.220^{+0.040}_{-0.040}$	$0.870^{+0.070}_{-0.060}$	$0.930^{+0.050}_{-0.050}$	$1.00^{+0.10}_{-0.10}$	19.9
K02607	5757^{+65}_{-65}	$4.460^{+0.060}_{-0.040}$	$0.130^{+0.040}_{-0.040}$	$0.990^{+0.080}_{-0.070}$	$1.030^{+0.050}_{-0.050}$	$1.70^{+0.20}_{-0.20}$	18.0
K02668	5489^{+66}_{-65}	$4.520^{+0.060}_{-0.040}$	$-0.080^{+0.040}_{-0.040}$	$0.860^{+0.070}_{-0.060}$	$0.900^{+0.040}_{-0.040}$	$1.40^{+0.10}_{-0.10}$	16.3
K02694	4816^{+65}_{-65}	$4.560^{+0.030}_{-0.040}$	$0.170^{+0.040}_{-0.040}$	$0.770^{+0.060}_{-0.060}$	$0.790^{+0.040}_{-0.040}$	$1.40^{+0.10}_{-0.10}$	20.2
K02753	5861^{+63}_{-57}	$4.190^{+0.080}_{-0.070}$	$0.170^{+0.040}_{-0.040}$	$1.400^{+0.160}_{-0.140}$	$1.100^{+0.060}_{-0.060}$	$1.20^{+0.10}_{-0.10}$	22.6
K02756	5908^{+64}_{-64}	$4.380^{+0.070}_{-0.070}$	$0.040^{+0.040}_{-0.040}$	$1.100^{+0.090}_{-0.090}$	$1.060^{+0.050}_{-0.050}$	$1.20^{+0.10}_{-0.10}$	16.1
K02763	4802^{+65}_{-63}	$4.590^{+0.030}_{-0.030}$	$-0.030^{+0.040}_{-0.040}$	$0.730^{+0.060}_{-0.050}$	$0.760^{+0.040}_{-0.040}$	$1.20^{+0.10}_{-0.10}$	12.0
K02796	5720^{+65}_{-65}	$4.400^{+0.070}_{-0.070}$	$-0.060^{+0.040}_{-0.040}$	$1.020^{+0.080}_{-0.080}$	$0.960^{+0.050}_{-0.050}$	$1.00^{+0.10}_{-0.10}$	13.0
K02874	5289^{+66}_{-62}	$4.450^{+0.070}_{-0.050}$	$-0.120^{+0.040}_{-0.040}$	$0.880^{+0.070}_{-0.060}$	$0.810^{+0.040}_{-0.040}$	$1.20^{+0.10}_{-0.10}$	8.4
K02875	4990^{+67}_{-67}	$4.570^{+0.040}_{-0.040}$	$-0.140^{+0.040}_{-0.040}$	$0.750^{+0.060}_{-0.060}$	$0.760^{+0.040}_{-0.040}$	$1.40^{+0.10}_{-0.10}$	7.2
K02879	5516^{+64}_{-68}	$4.510^{+0.070}_{-0.050}$	$-0.050^{+0.040}_{-0.040}$	$0.880^{+0.070}_{-0.070}$	$0.910^{+0.050}_{-0.050}$	$0.60^{+0.10}_{-0.10}$	8.2
K02916	4994^{+66}_{-67}	$4.550^{+0.030}_{-0.040}$	$-0.050^{+0.040}_{-0.040}$	$0.770^{+0.060}_{-0.060}$	$0.780^{+0.040}_{-0.040}$	$1.00^{+0.10}_{-0.10}$	7.4
K03009	5108^{+65}_{-63}	$4.560^{+0.050}_{-0.030}$	$0.090^{+0.040}_{-0.040}$	$0.810^{+0.060}_{-0.060}$	$0.850^{+0.040}_{-0.040}$	$1.00^{+0.10}_{-0.10}$	18.2
K03032	5186^{+62}_{-64}	$4.460^{+0.050}_{-0.060}$	$0.280^{+0.040}_{-0.040}$	$0.910^{+0.070}_{-0.070}$	$0.880^{+0.040}_{-0.040}$	$1.40^{+0.10}_{-0.10}$	15.4
K03065	5777^{+65}_{-65}	$4.510^{+0.040}_{-0.020}$	$-0.040^{+0.040}_{-0.040}$	$0.920^{+0.070}_{-0.070}$	$1.000^{+0.050}_{-0.050}$	$1.10^{+0.10}_{-0.10}$	21.6
K03246	4850^{+66}_{-66}	$4.580^{+0.040}_{-0.030}$	$0.090^{+0.040}_{-0.040}$	$0.760^{+0.060}_{-0.060}$	$0.790^{+0.040}_{-0.040}$	$0.80^{+0.10}_{-0.10}$	16.6
K03867	5554^{+62}_{-65}	$4.370^{+0.070}_{-0.080}$	$0.070^{+0.040}_{-0.040}$	$1.040^{+0.100}_{-0.090}$	$0.930^{+0.050}_{-0.050}$	$1.70^{+0.10}_{-0.10}$	22.6
K04002	5214^{+64}_{-65}	$4.540^{+0.050}_{-0.040}$	$0.130^{+0.040}_{-0.040}$	$0.830^{+0.070}_{-0.060}$	$0.880^{+0.040}_{-0.040}$	$1.30^{+0.10}_{-0.10}$	12.5
K04018	5468^{+65}_{-63}	$4.460^{+0.070}_{-0.070}$	$-0.070^{+0.040}_{-0.040}$	$0.920^{+0.070}_{-0.070}$	$0.880^{+0.040}_{-0.040}$	$1.30^{+0.10}_{-0.10}$	20.9
K04070	4937^{+62}_{-65}	$4.560^{+0.030}_{-0.040}$	$0.020^{+0.040}_{-0.040}$	$0.770^{+0.060}_{-0.060}$	$0.790^{+0.040}_{-0.040}$	$1.10^{+0.10}_{-0.10}$	19.0
K04072	5850^{+65}_{-61}	$4.250^{+0.080}_{-0.080}$	$0.060^{+0.040}_{-0.040}$	$1.260^{+0.130}_{-0.120}$	$1.050^{+0.050}_{-0.050}$	$1.00^{+0.10}_{-0.10}$	16.6
K04109	4987^{+63}_{-64}	$4.540^{+0.040}_{-0.040}$	$0.200^{+0.040}_{-0.040}$	$0.810^{+0.060}_{-0.060}$	$0.830^{+0.040}_{-0.040}$	$0.70^{+0.10}_{-0.10}$	15.8
K04159	5229^{+67}_{-69}	$4.460^{+0.040}_{-0.040}$	$0.060^{+0.040}_{-0.040}$	$0.890^{+0.070}_{-0.070}$	$0.830^{+0.040}_{-0.040}$	$0.80^{+0.10}_{-0.10}$	23.3
K04199	5122^{+65}_{-65}	$4.540^{+0.030}_{-0.040}$	$-0.210^{+0.040}_{-0.040}$	$0.780^{+0.060}_{-0.060}$	$0.760^{+0.040}_{-0.040}$	$0.80^{+0.10}_{-0.10}$	13.0
K04366	5330^{+65}_{-64}	$4.470^{+0.050}_{-0.050}$	$-0.190^{+0.040}_{-0.040}$	$0.860^{+0.070}_{-0.060}$	$0.800^{+0.040}_{-0.040}$	$1.30^{+0.10}_{-0.10}$	18.2
K04430	5126^{+65}_{-65}	$4.560^{+0.050}_{-0.030}$	$0.050^{+0.040}_{-0.040}$	$0.800^{+0.060}_{-0.060}$	$0.850^{+0.040}_{-0.040}$	$1.40^{+0.20}_{-0.20}$	12.2
K04441	4888^{+65}_{-65}	$4.560^{+0.030}_{-0.040}$	$0.010^{+0.040}_{-0.040}$	$0.760^{+0.060}_{-0.060}$	$0.780^{+0.040}_{-0.040}$	$1.40^{+0.20}_{-0.20}$	16.3
K04469	4930^{+65}_{-68}	$4.570^{+0.030}_{-0.040}$	$0.020^{+0.040}_{-0.040}$	$0.770^{+0.060}_{-0.060}$	$0.790^{+0.040}_{-0.040}$	$0.70^{+0.10}_{-0.10}$	21.4
K04746	5007^{+65}_{-65}	$4.570^{+0.040}_{-0.030}$	$0.060^{+0.040}_{-0.040}$	$0.780^{+0.060}_{-0.060}$	$0.820^{+0.040}_{-0.040}$	$0.80^{+0.10}_{-0.10}$	23.5
K04841	4803^{+67}_{-65}	$4.580^{+0.020}_{-0.030}$	$-0.170^{+0.040}_{-0.040}$	$0.710^{+0.060}_{-0.050}$	$0.710^{+0.040}_{-0.040}$	$1.30^{+0.10}_{-0.10}$	17.0
KIC8435766	5099^{+64}_{-69}	$4.590^{+0.020}_{-0.010}$	$-0.020^{+0.040}_{-0.040}$	$0.770^{+0.060}_{-0.060}$	$0.840^{+0.040}_{-0.040}$	$1.24^{+0.16}_{-0.16}$	8.5
KIC11187332	5579^{+65}_{-64}	$4.320^{+0.070}_{-0.070}$	$-0.170^{+0.040}_{-0.040}$	$1.060^{+0.110}_{-0.100}$	$0.870^{+0.040}_{-0.040}$	$1.30^{+0.12}_{-0.12}$	7.3
KIC2718885	5642^{+62}_{-63}	$4.370^{+0.080}_{-0.080}$	$0.070^{+0.040}_{-0.040}$	$1.060^{+0.100}_{-0.090}$	$0.960^{+0.050}_{-0.050}$	$1.13^{+0.19}_{-0.19}$	4.7

Table 2. Characteristics of "hot Jupiter" sample

ID	$T_{\rm eff}$ [K][a]	$\log g$[a]	[Fe/H][a]	$R_\star$ [$R_\odot$]	$M_\star$ [$M_\odot$]	R_p [$R_\oplus$]	$P_{\rm orb}$ [hr]
K00001	5795^{+67}_{-65}	$4.360^{+0.070}_{-0.070}$	$-0.050^{+0.040}_{-0.040}$	$1.080^{+0.100}_{-0.090}$	$0.980^{+0.050}_{-0.050}$	$14.50^{+1.20}_{-1.20}$	59.3
K00003	4887^{+64}_{-70}	$4.560^{+0.040}_{-0.030}$	$0.290^{+0.040}_{-0.040}$	$0.800^{+0.060}_{-0.060}$	$0.840^{+0.040}_{-0.040}$	$5.00^{+0.40}_{-0.40}$	117.4

Table 2 *(continued)*

ID	$T_{\rm eff}$ [K][a]	$\log g$[a]	[Fe/H][a]	$R_\star$ [$R_\odot$]	$M_\star$ [$M_\odot$]	R_p [$R_\oplus$]	$P_{\rm orb}$ [hr]
K00007	5846^{+68}_{-63}	$4.120^{+0.070}_{-0.070}$	$0.140^{+0.040}_{-0.040}$	$1.520^{+0.180}_{-0.160}$	$1.110^{+0.060}_{-0.060}$	$4.10^{+0.40}_{-0.40}$	77.0
K00017	5690^{+58}_{-62}	$4.230^{+0.070}_{-0.070}$	$0.330^{+0.040}_{-0.130}$	$1.330^{+0.140}_{-0.060}$	$1.100^{+0.060}_{-0.060}$	$13.80^{+1.40}_{-1.40}$	77.5
K00020	5987^{+67}_{-69}	$4.130^{+0.070}_{-0.080}$	$0.030^{+0.040}_{-0.150}$	$1.520^{+0.160}_{-0.050}$	$1.130^{+0.060}_{-0.060}$	$19.30^{+1.80}_{-1.80}$	106.6
K00022	5907^{+61}_{-62}	$4.210^{+0.070}_{-0.070}$	$0.170^{+0.040}_{-0.130}$	$1.380^{+0.150}_{-0.050}$	$1.120^{+0.060}_{-0.060}$	$14.00^{+1.30}_{-1.30}$	189.4
K00046	5694^{+57}_{-53}	$4.130^{+0.070}_{-0.080}$	$0.350^{+0.040}_{-0.160}$	$1.550^{+0.180}_{-0.080}$	$1.160^{+0.090}_{-0.080}$	$5.50^{+0.50}_{-0.50}$	83.8
K00063	5669^{+65}_{-65}	$4.510^{+0.030}_{-0.020}$	$0.200^{+0.040}_{-0.070}$	$0.940^{+0.080}_{-0.050}$	$1.030^{+0.050}_{-0.050}$	$6.00^{+0.50}_{-0.50}$	226.3
K00127	5587^{+69}_{-64}	$4.360^{+0.080}_{-0.080}$	$0.310^{+0.040}_{-0.100}$	$1.100^{+0.110}_{-0.050}$	$1.020^{+0.050}_{-0.050}$	$11.80^{+1.10}_{-1.10}$	85.9
K00128	5697^{+66}_{-65}	$4.230^{+0.070}_{-0.070}$	$0.230^{+0.040}_{-0.120}$	$1.300^{+0.130}_{-0.050}$	$1.040^{+0.050}_{-0.050}$	$14.20^{+1.30}_{-1.30}$	118.6
K00135	5968^{+66}_{-68}	$4.250^{+0.080}_{-0.070}$	$0.300^{+0.040}_{-0.140}$	$1.370^{+0.160}_{-0.060}$	$1.210^{+0.060}_{-0.060}$	$12.30^{+1.30}_{-1.30}$	72.5
K00141	5338^{+64}_{-63}	$4.440^{+0.070}_{-0.070}$	$0.270^{+0.040}_{-0.070}$	$0.960^{+0.080}_{-0.040}$	$0.930^{+0.050}_{-0.040}$	$5.60^{+0.50}_{-0.50}$	62.9
K00186	5818^{+64}_{-64}	$4.420^{+0.070}_{-0.060}$	$0.110^{+0.040}_{-0.080}$	$1.040^{+0.080}_{-0.050}$	$1.040^{+0.050}_{-0.050}$	$13.80^{+1.10}_{-1.10}$	77.8
K00201	5522^{+65}_{-69}	$4.260^{+0.070}_{-0.070}$	$0.290^{+0.040}_{-0.110}$	$1.220^{+0.120}_{-0.050}$	$0.990^{+0.050}_{-0.050}$	$10.60^{+0.90}_{-0.90}$	101.5
K00203	5726^{+64}_{-64}	$4.470^{+0.040}_{-0.030}$	$0.280^{+0.040}_{-0.070}$	$1.000^{+0.080}_{-0.050}$	$1.070^{+0.050}_{-0.050}$	$14.50^{+1.20}_{-1.20}$	35.8
K00214	5501^{+66}_{-68}	$4.380^{+0.080}_{-0.090}$	$0.370^{+0.040}_{-0.090}$	$1.070^{+0.100}_{-0.050}$	$1.010^{+0.050}_{-0.050}$	$10.30^{+0.90}_{-0.90}$	79.4
K00439	5448^{+64}_{-68}	$4.370^{+0.080}_{-0.080}$	$0.290^{+0.040}_{-0.090}$	$1.060^{+0.100}_{-0.040}$	$0.960^{+0.050}_{-0.050}$	$5.10^{+0.40}_{-0.40}$	45.6
K00466	5951^{+66}_{-67}	$4.140^{+0.080}_{-0.090}$	$-0.040^{+0.050}_{-0.150}$	$1.490^{+0.170}_{-0.050}$	$1.100^{+0.060}_{-0.050}$	$11.50^{+1.70}_{-1.70}$	225.4
K00760	5712^{+64}_{-67}	$4.360^{+0.080}_{-0.070}$	$0.010^{+0.040}_{-0.090}$	$1.070^{+0.100}_{-0.050}$	$0.970^{+0.050}_{-0.050}$	$12.40^{+1.00}_{-1.00}$	119.0
K00800	5866^{+65}_{-61}	$4.230^{+0.070}_{-0.070}$	$0.120^{+0.040}_{-0.120}$	$1.310^{+0.130}_{-0.050}$	$1.080^{+0.050}_{-0.050}$	$4.40^{+0.40}_{-0.40}$	65.0
K00870	4737^{+67}_{-66}	$4.600^{+0.030}_{-0.030}$	$-0.040^{+0.040}_{-0.050}$	$0.720^{+0.060}_{-0.040}$	$0.740^{+0.040}_{-0.040}$	$6.80^{+0.70}_{-0.70}$	215.8
K00889	5300^{+65}_{-64}	$4.490^{+0.060}_{-0.050}$	$0.160^{+0.040}_{-0.070}$	$0.890^{+0.070}_{-0.040}$	$0.890^{+0.040}_{-0.040}$	$11.60^{+0.90}_{-0.90}$	213.1
K00934	5506^{+58}_{-61}	$4.340^{+0.080}_{-0.090}$	$-0.200^{+0.040}_{-0.090}$	$1.020^{+0.100}_{-0.040}$	$0.840^{+0.040}_{-0.040}$	$4.20^{+0.30}_{-0.30}$	139.9
K01779	5855^{+63}_{-65}	$4.450^{+0.040}_{-0.030}$	$0.260^{+0.040}_{-0.080}$	$1.040^{+0.080}_{-0.050}$	$1.110^{+0.060}_{-0.050}$	$4.20^{+0.30}_{-0.30}$	111.8
K01800	5640^{+65}_{-66}	$4.520^{+0.040}_{-0.020}$	$0.030^{+0.040}_{-0.070}$	$0.900^{+0.070}_{-0.050}$	$0.980^{+0.050}_{-0.050}$	$6.20^{+0.60}_{-0.60}$	187.0

Table 3. Comparisons between metallicity distributions

Sample name	Number of stars	Sample mean [Fe/H]	p for comparison[a] with USPs	Hot Jupiters
USPs	62	0.0018 ± 0.0051	$\cdots$	1.8×10^{-4}
Hot Jupiters	25	0.1684 ± 0.0082	1.8×10^{-4}	$\cdots$
Hot Small Planets	242	0.0022 ± 0.0026	0.86	7.7×10^{-5}

[a] Probability of being drawn from the same distribution, based on a two-sample Kolmogorov-Smirnov test.